The application of adiabatic method for the description of impurity states in quantum nanostructures

2010 J. Phys.: Conf. Ser. 248 012047

(http://iopscience.iop.org/1742-6596/248/1/012047)

Journal of Physics: Conference Series **248** (2010) 012047 doi:10.1088/1742-6596/248/1/012047

The application of adiabatic method for the description of impurity states in quantum nanostructures

A. A. Gusev[1], O. Chuluunbaatar[1], S. I. Vinitsky[1], E. M. Kazaryan[2], H. A. Sarkisyan[2]

[1]Joint Institute for Nuclear Research, Dubna, Russia
[2]Russian-Armenian (Slavonic) University, Yerevan, Armenia

E-mail: gooseff@jinr.ru

Abstract. In the framework of effective mass approximation the application of adiabatic method for the description of impurity states in quantum dots, wires and wells with parabolic confinement potential as well as rectangular infinitely-high potential is presented. A rate of convergence of the method and efficiency of the proposed program complex for solving a boundary value problem, realized by the finite element method, is demonstrated on examples of calculation of spectral and optical characteristics of the considered quantum nanostructures.

1. Introduction

Investigations of the Coulomb systems in quantum nanostructures are important from the point of view of application of obtained results in a construction of semiconductor devices of a new generation. It is well known that by changing a dimension of the semiconductor structures the impurity binding energy is increasing. For this reason the influence of impurity states is more essential for low dimensional semiconductors. The impurity energy spectra in quantum well (QW), wire (QWr) and dot (QD) can be manipulated by external fields too [1]. Different methods of calculations of spectral characteristics and wave functions of impurities were applied in many papers.

The eigenvalue problem with both Coulomb potential and magnetic field is analytically not solvable, because the Schrödinger equation with appropriate boundary conditions is beyond the problem of confluent hypergeometric equations. Therefore it is necessary to use different approximation methods: variational, perturbation theory method, etc. In this regard it should be mentioned, that Maksym and Chakraborty on the base of numerical calculations obtained many-particle states in parabolic QD in external magnetic field and demonstrate the generalization of Kohn theorem for quantum nanostructures [2]. Jia-Lin Zhu et al using the method of series expansion have obtained the exact forms of series in different regions of the radial equation (a) for donor states in rectangular QW [3], (b) for two-dimensional hydrogenic donor states in magnetic field [4], (c) for two electrons confined by two-dimensional and three-dimensional QDs with parabolic potentials [5]. One of the powerful methods of the analytical solvation of similar problems is the adiabatic approximation. For the first time hydrogen-like system in adiabatic approximation was considered in connection with analysis of such system

behavior in extremely strong magnetic field [6]. A similar problem, but for electron with the relativistic dispersion law was solved in [7]. In [8] within the framework of the adiabatic theory the hydrogen-like impurity levels in spherical GaAs/$Ga_{1-x}Al_xAs$ QD with parabolic confinement potential under the influence of strong magnetic field are investigated. Variational and adiabatic methods were applied for study of impurity states in parabolic QWs [9, 10] and resonance effects of transmission and reflection at axial channeling of ions in parabolic QWrs or in magnetic field [11].

In this paper we continue the previous investigation in the framework of adiabatic method using elaborated symbolic-numerical algorithms [12, 13, 14] and program complex for solving the boundary value problems (BVPs), realized by the finite element method [15, 16, 17]. A rate of convergence of the method and efficiency of the proposed program complex is demonstrated on examples of calculation of spectral and optical characteristics of the considered quantum nanostructures.

2. Boundary value problems

In the effective mass approximation the Schrödinger equation for impurity electron in magnetic field in QD, QWr, QW is read as

$$\left\{\frac{1}{2\mu}\left(\hat{\vec{p}}-\frac{e}{c}\vec{A}\right)^2+U(\vec{r})-\frac{qe^2}{\kappa r_c}\right\}\Psi=E\Psi, \tag{1}$$

where $\mu=\beta m_e$ is the effective mass of electron, q is the Coulomb charge of impurity, $r_c=\sqrt{x^2+y^2+(z-z_c)^2}$ is the distance between electron and Coulomb charge of impurity center, $z_c\in[-z_0/2,z_0/2]$ is the shift of charge position q along z axis in the case of QW ($z_c=0$ for QD and QWr considered below), κ is the static dielectric constant of semiconductor (for GaAs $\beta=0.067,\quad q=1,\quad \kappa=13.18$), $U(\vec{r})$ is the parabolic potential with frequency $\omega=\gamma_{r_0}\hbar/(\mu\, r_0^2)$, $\gamma_{r_0}\sim\pi^2/3$ is an adjustable parameter (Model A):

$$U(\vec{r})\equiv U^{\mathrm{A}}(\vec{r})=\mu\omega^2(\zeta_1(x^2+y^2)+\zeta_3 z^2)/2, \tag{2}$$

$r_0=\sqrt{\zeta_1(x_0^2+y_0^2)+\zeta_3 z_0^2}$ is the radius of QD ($\zeta_1=1$, $\zeta_3=1$), QWr ($\zeta_1=1$, $\zeta_3=0$) and the depth of QW ($\zeta_1=0$, $\zeta_3=1$). For comparison we consider model QD, and QW ($\zeta_3=1/2$) with potential $U(\vec{r})$ (Model B)

$$\begin{aligned}U(\vec{r})&\equiv U^{\mathrm{B}}(\vec{r})=\{0,0\le|\vec{r}|<r_0;+\infty,|\vec{r}|\ge r_0\},\\ U(z)&\equiv U^{\mathrm{B}}(z)=\{0,|z|<z_0/2;+\infty,|z|\ge z_0/2\}.\end{aligned} \tag{3}$$

Choosing direction of z axis along the magnetic field $\vec{H}$ with vector potential $\vec{A}=\frac{1}{2}\vec{H}\times\vec{r}$ and using dimensionless parameter for magnetic field $\gamma=H/H_0^*$, and reduced atomic units (a.u.) (for GaAs $H_0^*=6$ T $a_B^*=102$ Å, $E_{au}=2E_R^*$, $E_R^*\equiv Ry^*=5.2$meV), we can rewrite (1) for given magnetic quantum number m in the following form

$$\begin{aligned}&\left(\frac{1}{g_{3s}(x_s)}\hat{H}_2(x_f;x_s)+\hat{H}_1(x_s)-2E\right)\Psi(x_f,x_s)=0,\\ &\hat{H}_2=-\frac{1}{g_{1f}(x_f)}\frac{\partial}{\partial x_f}g_{2f}(x_f)\frac{\partial}{\partial x_f}+\hat{V}_f(x_f)+\hat{V}_{fs}(x_f,x_s),\\ &\hat{H}_1=-\frac{1}{g_{1s}(x_s)}\frac{\partial}{\partial x_s}g_{2s}(x_s)\frac{\partial}{\partial x_s}+\hat{V}_s(x_s),\quad V_{fs}(x_f,x_s)=-\frac{2q}{\sqrt{\rho^2+(z-z_c)^2}}=-\frac{2q}{r_c}.\end{aligned} \tag{4}$$

Here $\hat{H}_2 \equiv \hat{H}_2(x_f;x_s) = g_{3s}(x_s)H_2(x_f;x_s)$ and $\hat{H}_1 \equiv \hat{H}_1(x_s) = H_1(x_s)$ are the Hamiltonians of so-called fast and slow subsystems, $\hat{V}_{fs}(x_f,x_s) = g_{3s}(x_s)V_{fs}(x_f,x_s)$ is the Coulomb potential in cylindrical or spherical coordinates (CC or SC). In the CC for QD and QWr we use the notations $x_f = \rho$, $x_s = z$, $g_{1f}(x_f) = g_{2f}(x_f) = \rho$, $g_{1s}(x_s) = g_{2s}(x_s) = g_{3s}(x_s) = 1$ (Model A):

$$\hat{V}_f(x_f) = m^2/\rho^2 + \gamma m + \gamma^2\rho^2/4 + \zeta_1\omega^2\rho^2, \quad \hat{V}_s(x_s) = \zeta_3\omega^2 z^2.$$

while for QW $x_f = z$, $x_s = \rho$, $g_{1f}(x_f) = g_{2f}(x_f) = 1$, $g_{1s}(x_s) = g_{2s}(x_s) = \rho$, $g_{3s}(x_s) = 1$,

$$\hat{V}_f(x_f) = \zeta_3\omega^2 z^2, \quad \hat{V}_s(x_s) = m^2/\rho^2 + \gamma m + \gamma^2\rho^2/4 + \zeta_1\omega^2\rho^2.$$

In the SC we use the notation $x_f = \eta_c$, $x_s = r_c$, $g_{1f}(x_f) = 1$, $g_{2f}(x_f) = (1-\eta_c^2)$, $g_{1s}(x_s) = g_{2s}(x_s) = r_c^2$, $g_{3s}(x_s) = r_c^2$ (Model A)

$$\hat{V}_f(x_f) = m^2/(1-\eta^2) + 2p\gamma m + \alpha(1-\eta_c^2) - b\eta_c + f, \quad \hat{V}_s(x_s) = \beta r_c^4,$$

where $\alpha = p^2$, $p = \gamma r_c^2/2$, $b = f = 0$, $\beta = \omega^2$ for QD ($\beta = 0$ for QWr) and $\alpha = -c^2$, $c = \omega r_c^2$, $b = -2\omega z_c r_c^3$, $f = \omega z_c r_c^2$, $\beta = 0$, $\gamma = 0$ for QW.

The required solution of (4) we find in the form of expansion over a set of solutions, $\Phi_j(x_f;x_s)$,

$$\Psi_i(x_f,x_s) = \sum\nolimits_{j=1}^{j_{\max}} \Phi_j(x_f;x_s)\chi_j^{(i)}(x_s), \tag{5}$$

of the parametric eigenvalue problem of the fast subsystem in domain $\Omega_f = (x_f^{min}, x_f^{max})$

$$\left\{\hat{H}_2(x_f;x_s) - \hat{E}_i(x_s)\right\}\Phi_i(x_f;x_s) = 0, \quad \langle\Phi_i|\Phi_j\rangle_{\Omega_f} = \int_{x_f^{\min}}^{x_f^{\max}} \Phi_i(x_f;x_s)\Phi_j(x_f;x_s)g_{1f}(x_f)dx_f = \delta_{ij}. \tag{6}$$

Substituting expansion (5) in eq. (4) and taking into account (6), we come to the BVP for a set of the differential equations of the slow subsystem related to the vector-function $\boldsymbol{\chi}^{(i)}(x_s) = \{\chi_j^{(i)}(x_s)\}_{j=1}^{j_{\max}}$:

$$\mathbf{H}\boldsymbol{\chi}^{(i)}(x_s) = 2E_i\,\mathbf{I}\boldsymbol{\chi}^{(i)}(x_s), \tag{7}$$

$$\mathbf{H} = -\frac{1}{g_{1s}(x_s)}\mathbf{I}\frac{d}{dx_s}g_{2s}(x_s)\frac{d}{dx_s} + \hat{V}_s(x_s)\mathbf{I} + \mathbf{U}(x_s) + \frac{g_{2s}(x_s)}{g_{1s}(x_s)}\mathbf{Q}(x_s)\frac{d}{dx_s} + \frac{1}{g_{1s}(x_s)}\frac{dg_{2s}(x_s)\mathbf{Q}(z)}{dx_s}.$$

Here $\mathbf{I}$, $\mathbf{U}(x_s) = \mathbf{U}^T(x_s)$ and $\mathbf{Q}(x_s) = -\mathbf{Q}^T(x_s)$ are **unit, symmetric and nonsymmetric** matrixes with dimensions $j_{\max} \times j_{\max}$:

$$U_{ij}(x_s) = \frac{1}{g_{3s}(x_s)}\hat{E}_i(x_s)\delta_{ij} + \frac{g_{2s}(x_s)}{g_{1s}(x_s)}W_{ij}(x_s), \tag{8}$$

$$Q_{ij}(x_s) = -\langle\Phi_i(x_s)|\frac{\partial\Phi_j(x_s)}{\partial x_s}\rangle_{\Omega_f}, \quad W_{ij}(x_s) = \langle\frac{\partial\Phi_i(x_s)}{\partial x_s}|\frac{\partial\Phi_j(x_s)}{\partial x_s}\rangle_{\Omega_f}.$$

Solutions of discrete spectrum were subjected to the following boundary conditions:

$$\lim_{x_s\to x^{\min}=0} g_{2s}(x_s)\frac{d\boldsymbol{\chi}^{(i)}(x_s)}{dx_s} = 0,\ \boldsymbol{\chi}^{(i)}(x_s^{\max}) = 0; \quad \text{and} \quad \boldsymbol{\chi}^{(i)}(x_s^{\min}) = 0, \quad \boldsymbol{\chi}^{(i)}(x_s^{\max}) = 0, \tag{9}$$

for $x_s = \rho$ or $x_s = r$, and $x_s = z$, respectively, and orthonormalization conditions

$$\int_{x_s^{\min}}^{x_s^{\max}} (\boldsymbol{\chi}^{(i)}(x_s))^T\boldsymbol{\chi}^{(j)}(x_s)g_{1s}(x_s)dx_s = \delta_{ij}. \tag{10}$$

For Model B we have potentials $\hat{V}_s(x_s) = 0$ and $\hat{V}_f(x_f) = 0$ and use: conditions (9) for $r_{\max} = r_0$ if (7), (10) for the case of QD, and the last conditions (9) for $s \leftrightarrow f$, $z_{\min} = -z_0/2$, $z_{\max} = z_0/2$ if (6) for the case of QW. Presented below results of solving the BVPs (4)–(10) in the SC and CC are found by means of complex of programs ODPEVP, POTHMF and KANTBP [15, 16, 17].

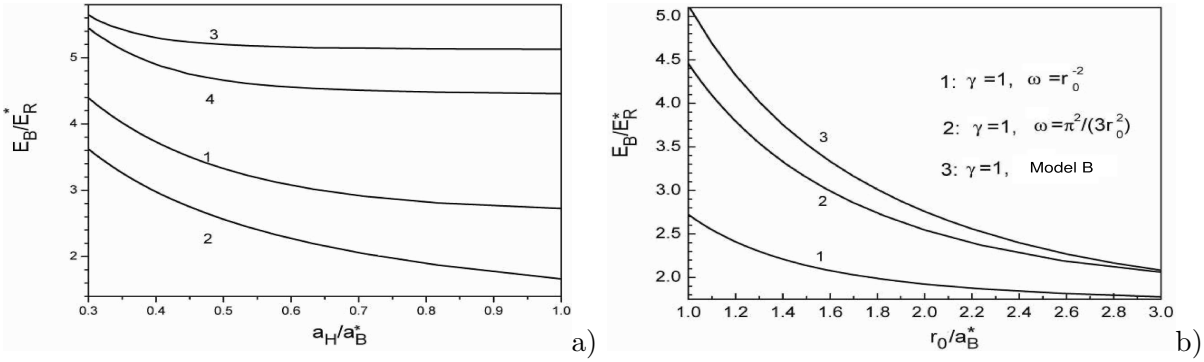

Figure 1. a) Binding energy of ground state electron E_B/E_R^* vs magnetic length $a_H^*/a_B^* = 1/\sqrt{\gamma}$ ($1 \le \gamma \le 11$) for $q = 1$, $m = 0$ and fixed radius of QD $r_0 = a_B^*$: 1 and 4 impurity electron (Model A) with confined potential frequencies $\omega = 1/r_0^2$ and $\omega = \pi^2/(3r_0^2)$; 3 is impurity electron in QD (Model B); 2 is impurity electron (Model A) without confined potential ($\omega = 0$). b)Binding energy of ground state electron E_B/E_R^* vs radius of QD at fixed magnetic field $\gamma = 1$.

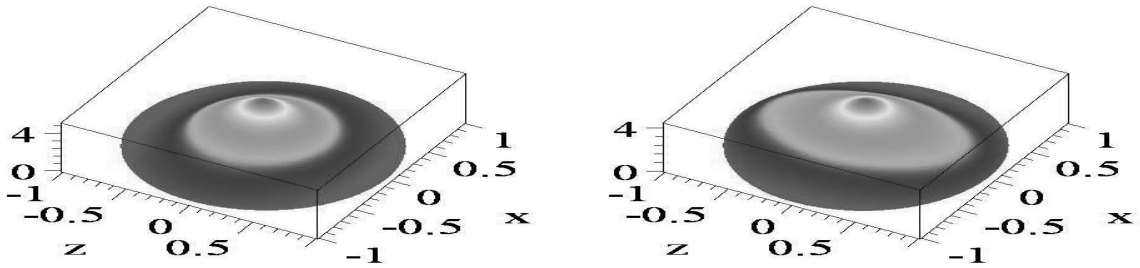

Figure 2. The profile of wave functions of the ground impurity states of QD with radius $r_0 = 1$ (Model B) in plane zx at magnetic field: $\gamma = 1$(left panel) and $\gamma = 10$(right panel).

3. Results and discussions

Determining binding energy of impurity as difference between electron without impurity center in QD E_0 ($q = 0$) and with one $E_1(q = 1)$, we can write $E_B = E_0 - E_1$. On Figs. 1a and 1b we show dependencies of the binding energies $E_B\,(a_H)$ at fixed radius of QD $r_0 = a_B^*$ and $E_B\,(r_0)$ at fixed magnetic field $H = H_0^* = 6$ T. As one can see from Fig. 1a with increasing H (decreasing magnetic length $a_H = a_B^*/\sqrt{\gamma}$) binding energy is increased, because the problem transforms to one-dimensional one. From Fig. 1b one can see, that with decreasing r_0 binding energy $E_B(r_0)$ is increased, because of reducing domain of localization of the electron probability density around the impurity center. From comparison of curves 1, 4 3 on Fig. 1a, and curves 1, 2 and 3 on Fig. 1b follows, that choosing value of parameter $\gamma_{r_0} = \pi^2/3$ provides quality agreement of models A and B. This fact connected with transforming of the discussed problem for QD as well as QWr to the problem of one dimensional hydrogen system. It is illustrated by the distributions of the wave functions of the ground state impurity electron in QD and QWr on Figs. 2 and 3, respectively.

On Fig. 4a we show the dependencies of binding energy of of the ground state impurity electron $E_B/(2E_R^*)$ in QWr without confinement potential ($\omega = 0$), versus magnetic field $\gamma = H/H_0^*, H_0^* = 6$T, that were calculated in different approximations and parametrizations of the problem (1) in the SC and CC. Curve 1 show values of E_B, i.e., $\mathcal{E}_1 = \gamma - 2E_1$, that where calculated by solving the BVP for (7)–(10) in the SC with $j_{max} = 10$ at a given accuracy (GA), which here was chosen as $\sim 10^{-8}$. Note, in interval $1 \le \gamma \le 11$ curve 1 corresponds to curve 2 on Fig. 1. Curves 4 and 5 show upper and lower estimations of binding energy, $E_{AD;c}^C$

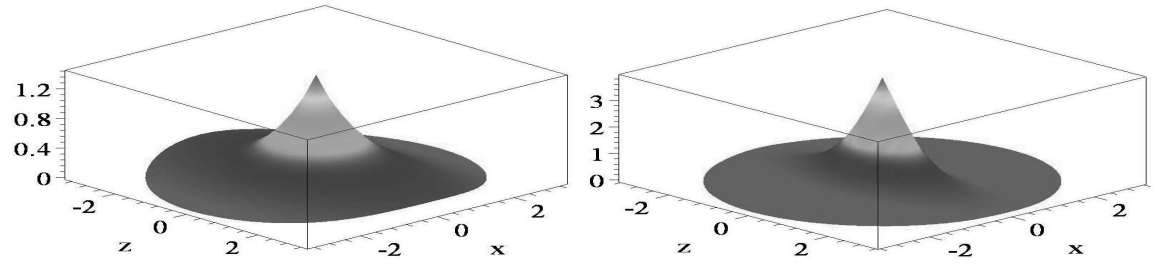

Figure 3. The profile of wave functions of ground impurity state in QWr without confinement potential($\omega = 0$) (Model A)in plane zx at magnetic field: $\gamma = 1$(left panel) and $\gamma = 10$(right panel).

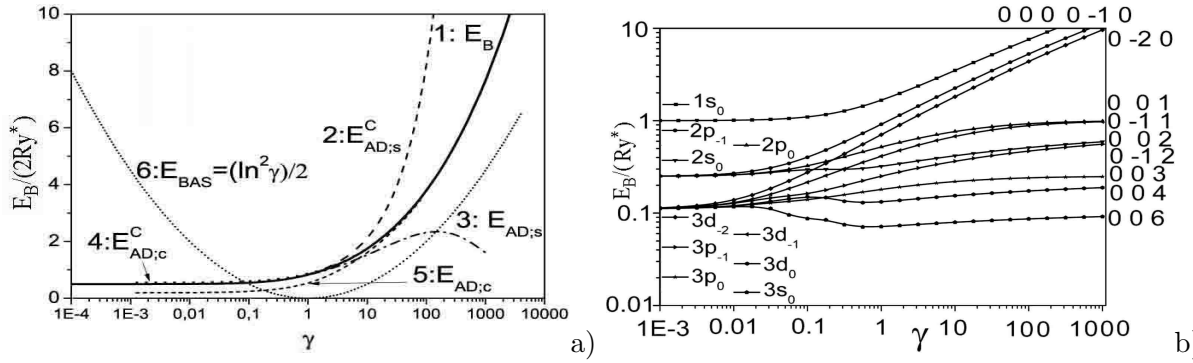

Figure 4. (a) The ground binding energy $E_B/(2E_R^*)$ of QWr (Model A) vs magnetic field $\gamma = H/H_0^*, H_0^* = 6$T in different approximation. (b) The first ten values of binding energy (in Ry*) levels $E_B/E_R^* = \mathcal{E}_i = \gamma - 2E_i$ classified by adiabatic sets of quantum numbers: spherical (N, l, m) for small γ and cylindrical (N_ρ, m, N_z) for large γ ones at $m \leq 0$, vs magnetic filed γ.

and $E_{AD;c}$, that where calculated by solving the BVP for (7) in the CC at $j_{max} = 1$ in a crude adiabatic approximation (CAD) at $W_{11} = 0$ and conventional adiabatic approximation (AD)at $W_{11} \neq 0$. One can see that these estimations go to curve 1 of the GA starting with $\gamma \geq 50$. For the interval of values $\gamma < 1$ the convergence rate of expansion (5) in the CC is slow, because conditions of the Kato type in a vicinity of point $z = 0$ does not fulfill [11].

Correspondingly, curves 2 and 3 show the upper and lower estimations of binding energy, $E^C_{AD;s}$ and $E_{AD;s}$, that were calculated by solving BVP for (7) in the SC at $j_{max} = 1$ in the CAD and the AD. One can see that these estimations approach to the values calculated with the GA (curve 1) starting from $\gamma < 1$ and remove from the GA values starting from $\gamma > 1$. However, for expansion (5) in the SC conditions of the Kato type near a vicinity of point $r = 0$ are satisfied, that leads to the high rate of convergence of such expansion and allows us to limit the same $j_{max} = 10$ for $1 < \gamma \leq 1000$ too [17]. For example, on Fig. 4b we show a behavior of the first ten values of binding energy (in Ry*) levels $\mathcal{E}_i = \gamma - 2E_i$ calculated with the GA in the SC and classified by adiabatic sets of quantum numbers: spherical (N, l, m) for small γ and cylindrical (N_ρ, m, N_z) for large γ at $m \leq 0$, vs magnetic field γ.

Note, if one describes the impurity states in QD, QWr and QW in strong magnetic field, on the first glance, it is possible to consider Coulomb interaction in problem (1) as small perturbation in the CC, and to use a well known estimation with logarithmic accuracy $E_{BAS} \simeq (\ln^2 \gamma)/2$ like in the case of ground state of a hydrogen atom in a strong magnetic field [18]. However from Fig. 4a one can see that there is three a times difference of the logarithmic estimation (curve 6) with respect to curve 1 of the GA. This question is discussed in details in [19].

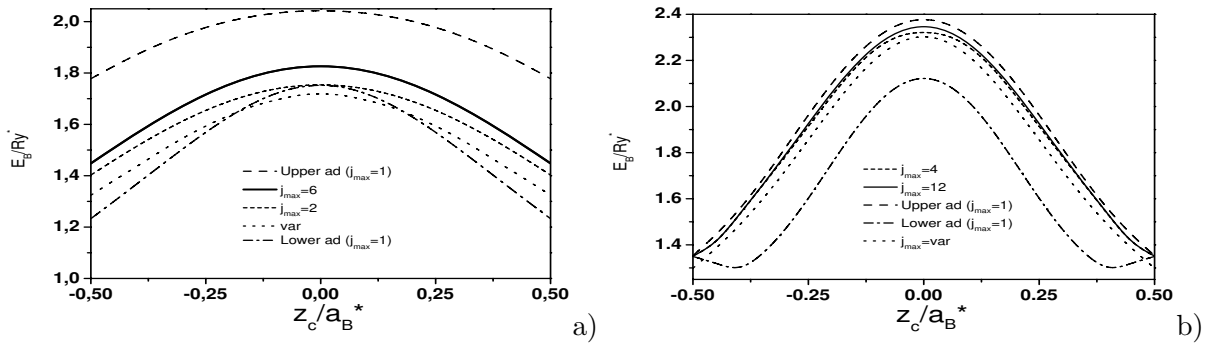

Figure 5. Binding energy $E_B/Ry^* = E_1^{th} - 2E_1(z_c)$ of QW vs position of Coulomb impurity z_c and number of basis functions $j_{\max}$, and crude adiabatic approximation (upper ad), adiabatic approximation (lower ad), and variational calculation (var): (a) Model A at $q = 1$, $m = 0$, $\omega = 3$, $E_1^{th} = \omega$ in the SC, and (b) Model B $q = 1$, $m = 0$, $z_0 = 1$, $E_1^{th} = \pi^2/z_0^2$ in the CC.

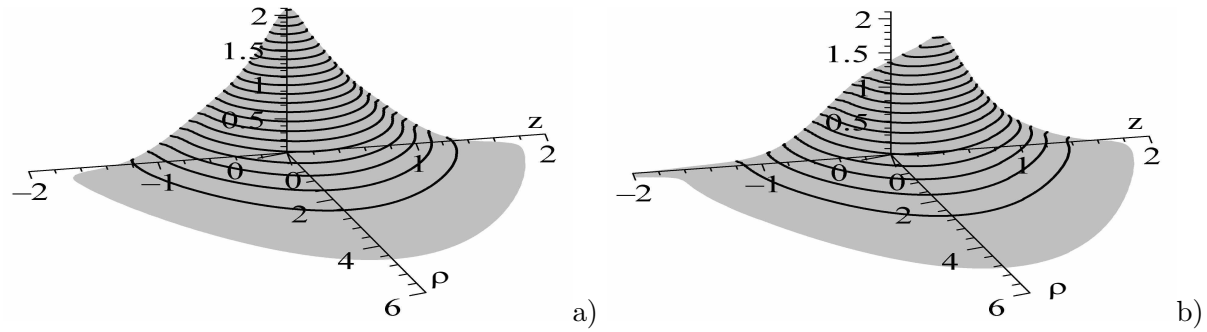

Figure 6. The profile of wave function of ground impurity state in QW (Model A) in plane zx at $q = 1$, $m = 0$, $\omega = 3$ and shift Coulomb center: (a) $z_c = 0$ and (b) $z_c = 0.4$.

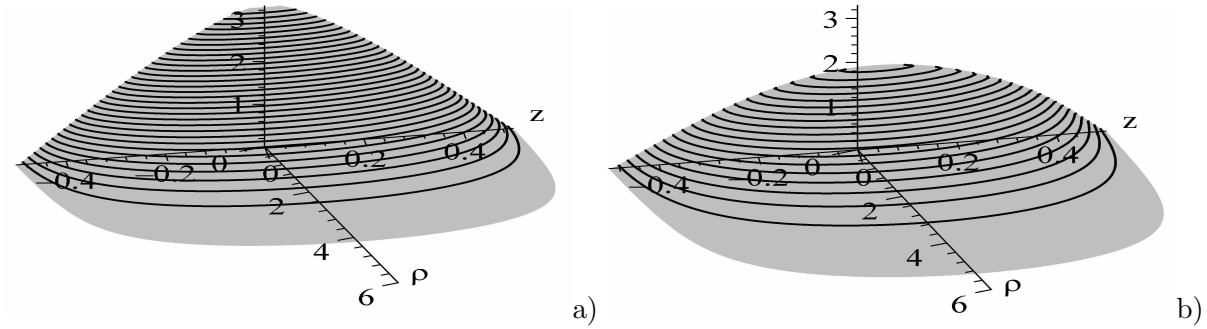

Figure 7. The profile of wave function of ground impurity state in QW (Model B) in plane zx at $q = 1$, $m = 0$, $z_0 = 1$ and shift Coulomb center: (a) $z_c = 0$ and (b) $z_c = 0.4$.

On Fig. 5 the upper and lower estimations of binding energy E_B of the ground state impurity electron in QW without magnetic field, correspondingly, for model A in the SC and model B in the CC, connected with impurity position z_c, as well as convergence by number j_{max} of basis functions in expansion (5) and their comparison with variational estimation are demonstrated. As it follows from Fig. 5, expansion (5) in the CC has a lower convergence rate with respect to one in the SC by the same reason [10] as for the QWr mentioned above. Fig. 6 and Fig. 7 show the wave functions of ground state of impurity electron in QW, for model A and B, respectively.

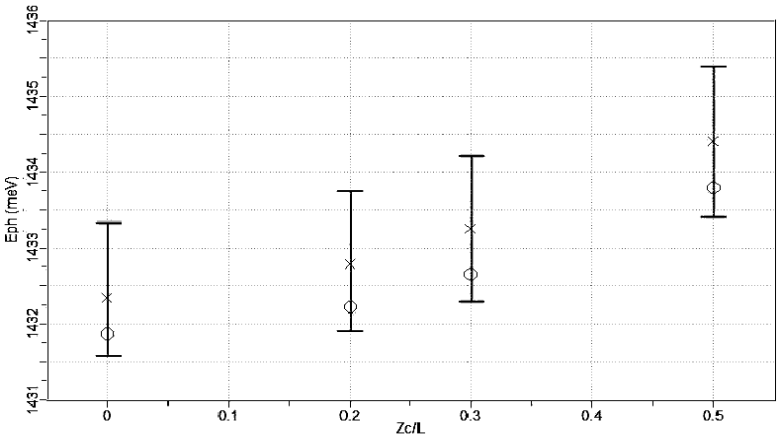

Figure 8. The interval of the resonance photon energy (in meV) $E_{ph} = \hbar\omega_{ph} = E_f - E_i$ determines the peak values of the absorption coefficient $K(\omega_{ph})$ vs the position of the impurity center z_c/L, $L = 102$Å: the vertical intervals are upper and lower adiabatic estimates, the crosses are variational estimates, the circles are estimates with given accuracy.

For the case of QW with parabolic confinement the coordinate of the maximum value of wave function coincide with the coordinate of impurity center. On the other hand, for Model B, due to Dirichlet boundary conditions in points $z_{\min} = -1/2$, $z_{\max} = 1/2$, the maximum of wave function is in a vicinity of the central point. Differences in the behavior of these wave functions allows us to verify models A and B.

Obtained estimations allow us to reveal the possible boundary of intervals of the photon resonance energies $E_{ph} = \hbar\omega_{ph}$ presented. For example, on Fig. 8, it is illustrated the maximal value of absorption coefficient $K(\omega_{ph})$ dependent upon the position of impurity in QW [9]. Based on the results for wave functions and eigenvalues it is possible to calculate impurity and inter impurity absorption coefficient for QD, QWr and QW. The impurity absorption coefficient $K(\omega)$ in parabolic GaAs QW is calculated with the help of variational functions [9]:

$$K(\omega_{ph}) = \frac{4\pi^2 e^2}{\kappa m_0^2 c \omega_{ph} V} \sum_{i,f} \left|\vec{e}\vec{M}_{if}\right|^2 \delta(E_f - E_i - \hbar\omega_{ph}), \qquad (11)$$

where V is the volume of a sample, $\vec{e}$ is the light polarization vector, $\vec{M}_{if}$ is the matrix element of the transition from the initial state i to the final one f, E_i and E_f are the energies of the initial and final states, delta-function provides the conservation of energy in the course of the transitions. Fig. 9a shows the absorption curves for transitions related to acceptors and donors. We can see, the strong difference exists between the shape of absorption curves, corresponding to donor and acceptor levels. During transitions between the acceptor level and conductive band the denominator of Eq. (11) at small values of wave vectors is close to unity, as far as for GaAs the ratio $m_c/m_v \approx 0.1$, therefore the absorption coefficient depending on the energy of incident photon has step-like feature, thus repeating the behavior of density of states. The absorption scenario related to donors is different. While increasing the denominator in Eq. (11) at a quite small interval from the absorption threshold the absorption rapidly decreases ($m_c/m_v \approx 9.25$).

Figure 9b shows the dependence of the blue shift on different values of two-dimensional concentrations of dominant impurity (acceptor). The difference between acceptor and donor energy levels can be presented as $E_{DAP} = E_{gap} + E_{bD} + E_{bA} + e^2/R$, where E_{bD} and E_{bA} are donor and acceptor binding energies, respectively; the fourth item in E_{DAP}, i. e. e^2/R, is the Coulomb term. In the frameworks of our calculations the blue shift $\Delta E_{blueshift}$ is proportional to the Coulomb term, i. e. inversely proportional to the distance between donor and acceptor $\Delta E_{blueshift} = e^2/R$. When the acceptor concentration is increasing (e. g. the concentration of Si atoms [20]), donors (e. g. residual C atoms [20]) and acceptors become spatially closer, the blue shift in the acceptor–donor transition peak takes place as a result of the increase of the Coulomb term [22, 20]. So, the growth of doping level is the reason for the increase of the blue shift.

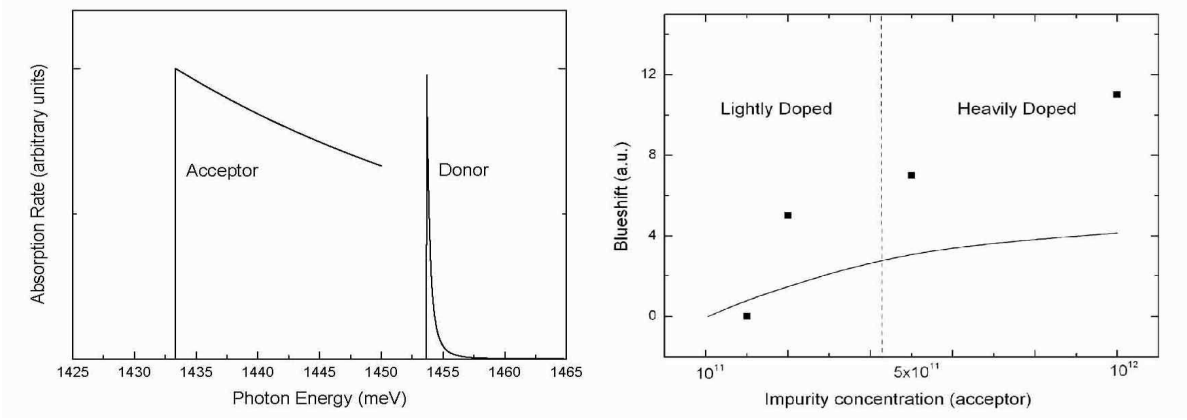

(a) (b)

Figure 9. a) The difference of absorbtion for transitions "conduction band → acceptor band" (Acceptor) and "valence band → donor band" (Donor) at L=100Å, $m_v/m_c = 9.\ 2$ (in GaAs QW). b) The dependence of the blue shift (in a.u.) for transitions donor-acceptor vs concentration of dominant (acceptor) impurity (after the averaging between D–A distance): squares are experimental results [20], solid line is result of calculations [21], the left panel shows the domain of low concentration, the right one shows the domain of high concentration.

4. Conclusion

In this paper we demonstrate effective methods of calculation of impurity states in the present magnetic field for cases of QW, QWr and QD. As result of our investigation we can say that adiabatic approach is good mechanism for describing the Coulomb systems in quantum nanostructures. There are good agreement between adiabatic and variational procedures of calculation of energy spectra and wave functions of impurities in QW, QWr, QD.

Authors thank Profs. V. L. Derbov, V. P. Gerdt, A. A. Kostanyan and V. V. Serov for collaboration. The work was supported partially by RFBR (grants 10-01-00200 and 08-01-00604) and by the grant No. MK-2344.2010.2 of the President of Russian Federation.

[1] Miura N 2008 *Physics of semiconductors in high magnetic fields* (New York, Oxford Univ. Press Inc)
[2] Maksym P A and Chakraborty T 1990 *Phys. Rev. Lett.* **65** 108.
[3] J -L Zhu 1989 *Phys. Rev. B* **39** 8780
[4] J -L Zhu, Y Cheng and J -J Xiong 1990 *Phys. Rev. B* **41** 10792.
[5] Zhu J -L, Li Z -Q, Yu J -Z, Ohno K and Kawazoe Y 1997 *Phys. Rev. B* **55** 15819
[6] Elliott R and Loudon R 1959 *J. Phys. Chem. Sol.* **8** 382
[7] Avetisyan A A et al 1999 *Phys. Stat. Sol. B* **214** 91
[8] Kazaryan E M, Petrosyan L S and Sarkisyan H A 2001 *Int. J. Mod. Phys. B* **15** 4103
[9] Kazaryan E M et al 2005 *Physica E* **28** 423
[10] Gusev A A et al 2010 *Phys. At. Nucl.* **73** 331
[11] Chuluunbaatar O et al 2009 *Phys. At. Nucl.* **72** 811
[12] Gusev A A et al 2010 *Math. Comput. in Simulation* (accepted); arXiv:1005.2089v1 [cond-mat.mes-hall]
[13] Gusev A A et al 2010 *Lect. Notes in Comput. Sci.* **6244** 106; arXiv:1004.4202v1 [cond-mat.mes-hall].
[14] Vinitsky S I et al 2009 *Lect. Notes in Comput. Sci.* **5743** 334
[15] Chuluunbaatar O et al 2009 *Comput. Phys. Commun.* **180** 1358
[16] Chuluunbaatar O et al 2008 *Comput. Phys. Commun.* **178** 301
[17] Chuluunbaatar O et al 2008 *Comput. Phys. Commun.* **179** 685
[18] Landau L D and Lifshitz E M 1977 *Quantum Mechanics, 3rd ed* (Oxford, Pergamon)
[19] Karnakov B M and Popov V S 2003 *J. Exp. Theor. Phys.* **97** 890
[20] Guzman A et al 1999 *IEE Proceedings Optoelectronics* **146** 89
[21] Kazaryan E M, Kostanyan A A and Sarkisyan H A 2007 *J. Phys. Cond. Mat.* **19** 046212
[22] Ding Y J, Korotkov R, Khurgin J B, Rabinovich W S and Katzer D S 1998 *Appl. Phys. Lett.* **72** 534